JOURNAL OF APPLIED ELECTROCHEMISTRY 6 (1976) 127–134

A special type of Raney-alloy catalyst used in compact biofuel cells

U. GEBHARDT, J. R. RAO, G. J. RICHTER

Forschungslaboratorien der Siemens AG, Erlangen, Germany

Received 29 January 1975

In developing implantable biofuel cells to generate higher power it is essential to prepare very thin and highly active electrodes in order to produce the required energy in as small a volume as possible. A method has been developed for glucose electrodes which enables us to produce firmly adhering active layers on very thin foils (up to 50 μm) of homogeneous alloys, containing platinum and a ferrous metal, by controlled anodic dissolution of the non-noble metal. Such electrodes are roughly 10 to 20 times more active than conventional glucose anodes. The activity is remarkably increased by the addition of tungsten and tantalum to the alloy. So far it has been possible to transfer 17 out of the 24 available electrons of the glucose molecule.

1. Introduction

In the attempts to develop an implantable glucose-oxygen cell as an energy source for an artificial blood pump, the main problem is to find ways and means of preparing very thin and highly active glucose electrodes which permit generation of the required energy in the smallest possible volume. Raney noble metal catalysts supported on a metal foil have offered a reasonable solution to the problem of anodes.

In order to produce thin active layers on a nickel sheet, aluminium was deposited on nickel from a metal-organic electrolyte, and under defined conditions of temperature allowed to diffuse into nickel [1]. Discrete phases of $NiAl_3$ and Ni_2Al_3 in thin surface layers were thus created. Aluminium could be extracted from these film-like phases in the usual manner with potassium hydroxide, resulting in the formation of active surface layers on the metal foil.

We used platinum instead of nickel, and a ferrous metal such as iron, cobalt or nickel instead of aluminium. This choice has some advantages which extend beyond the specific case in question.

2. Preparation of anode foils from noble metal alloys

There are several possibilities of preparing metal alloy foils for the Raney method. Two cases will be described in detail here.

2.1. *Diffusion of a non-noble partner into the platinum metal*

Nickel is galvanically deposited on a platinum foil of a thickness of approximately 100 μm until the layer thickness attains 150 μm on both sides. The mutual diffusion of platinum into nickel and vice versa is enhanced by annealing at almost the melting point of nickel.

Fig. 1 represents the concentration curves of platinum and nickel over the cross-section of the foil after the deposition of nickel on platinum (a), after a 2 h annealing at 1450°C (b), and again after extraction of the nickel (c). The three recordings are comparable only qualitatively because they were not made with the same sample. The concentration variation was determined by the microprobe. A longer annealing period naturally results in an equidistribution of the components over the entire cross-section. But a supporting metal layer in the middle is just desirable. The sample is activated by etching with a drop of a hot mixture containing 50 ml concentrated nitric acid, 25 ml water and 25 ml concentrated sulphuric acid and allowed to react for 30 min. It was found that the concentrations in the interior had not changed. Thus with a nickel content below 50–60% the alloy can no

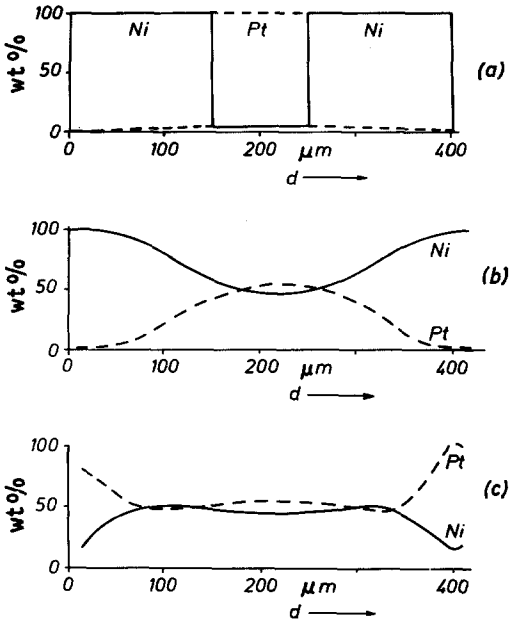

Fig. 1. Concentration curves over the cross-sections of platinum-nickel foils. (a) Before annealing; (b) after a 2 h annealing at 1450°C; (c) after the activation.

longer be activated by this method. On the contrary, nickel is dissolved in the boundary regions, leaving behind active platinum. Fig. 2 shows the micrograph of an etched sample. It is remarkable that only the boundary regions obtained from the nickel-rich alloys were strongly cracked and tended to break, whilst the interior active zone appeared uniformly black and obviously adhered well to the non-active metallic core.

2.2. *Preparation from a fusible regulus*

In other cases we proceeded directly with defined mixtures of noble metal and ferrous metal to obtain the alloys. For experimental purposes the ground samples were surface-activated or the alloy was rolled down to a thin foil and likewise surface-activated or activated completely. Unlike the aluminium alloys, such sheets are very elastic and easy to handle, but cannot be leached with potassium hydroxide in the usual manner.

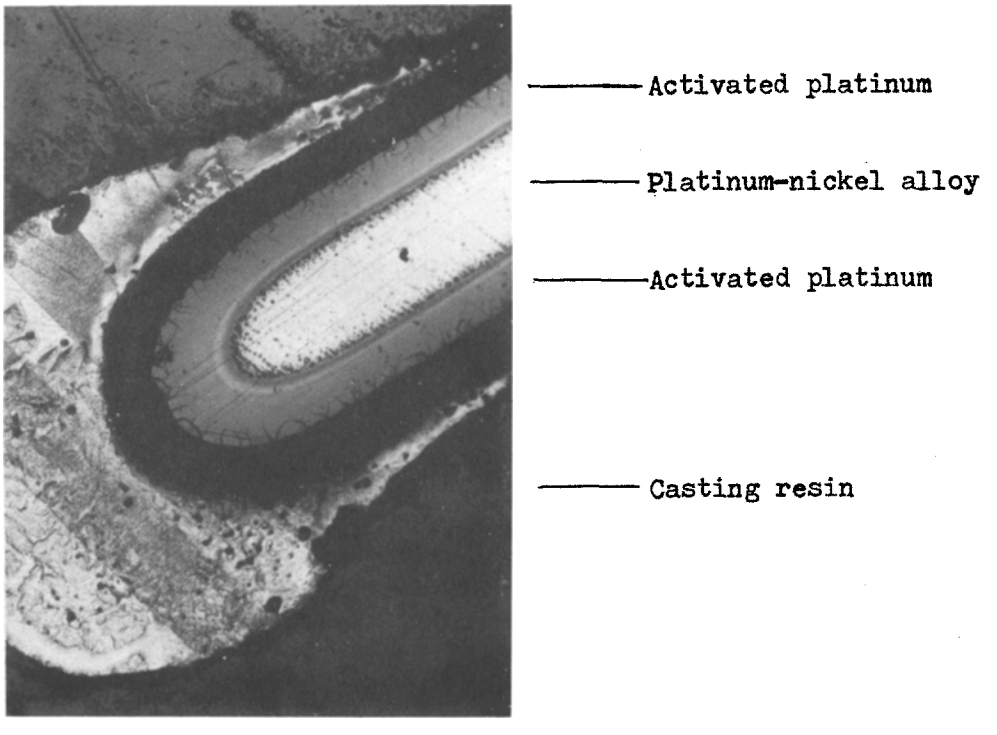

Fig. 2. Micrograph of an activated platinum-nickel foil.

3. Extraction of the ferrous metal

The various possible means of activation include chemical as well as electrochemical methods, such as galvanostatic,potentiodynamic and potentiostatic ones. The potentiostatic method has proved to be the best of these.

The galvanostatic method leads to poorly adhering layers which peel off; the potentiodynamic method produces deep cracks along the grain boundaries; but the potentiostatic method yields well-adhering active layers in the potential range between 400 and 800 mV (RHE) at 80°C in 1 M H_2SO_4. Besides, this method allows us to control the thickness of the active layer by passing a defined charge.

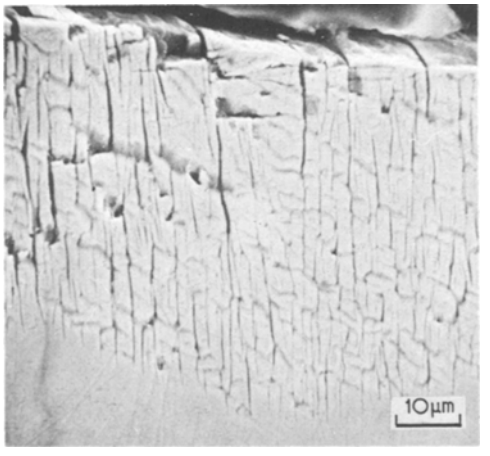

Fig. 3. Scanning electron-micrograph of Pt–Fe electrode; Pt : Fe = 1 : 3; potentiostatically activated in 1 M H_2SO_4; thickness of the active layer: 55 µm.

Fig. 3 shows the scanning electron micrograph of the active layer of a platinum-iron alloy (atomic ratio 1:3). The thickness of the layer is 55 µm. The micropores responsible for the activity have not been resolved even at this magnification. Their radii are approximately 2 nm. Only the secondary macropores are visible which here are oriented perpendicularly to the surface. There are hardly any cracks parallel to the surface. That is the reason for the good adherence of the active layer on the metallic support. These active layers are in fact surprisingly strong and are hardly damaged by scraping.

The porosity is naturally dependent on the

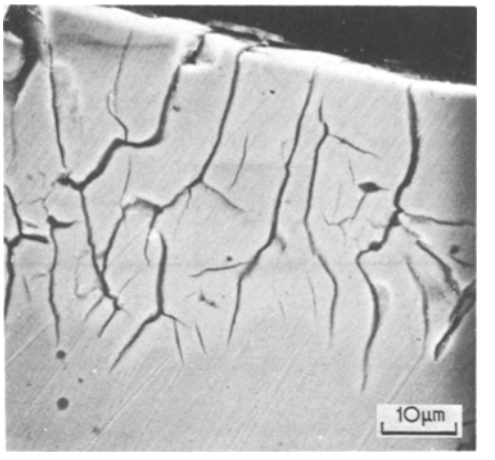

Fig. 4. Scanning electron-micrograph of Pt–Fe electrode; Pt : Fe = 1 : 3; potentiostatically activated in 1 M HCl; thickness of the active layer: 44 µm.

ferrous metal content of the starting alloy. It is surprising that the electrolyte in which the activation process is conducted also has a marked influence on the porous structure. This can be clearly distinguished on a macroscopic scale by comparing Fig. 3 with Fig. 4. The potentiostatic treatment was carried out in sulphuric acid in the former and in hydrochloric acid in the latter case.

3.1. *The amount of ferrous metal in the alloy after extraction*

The amount of the non-noble metal left behind after the anodic dissolution process is dependent on the nature and amount of the ferrous metal employed in preparing the homogeneous alloys. In the case of a Pt–Ni alloy with an atomic ratio of 1:6 (the proportions of all the metals are expressed in terms of their atomic ratios), nickel left behind after extraction was determined to be 7·2%. In a Pt–Ni alloy with a ratio of only 1:4, 15·9% of Ni remains behind. In general the amount of nickel present after the anodic dissolution process is low when the starting alloy contains a lower atomic ratio of the noble metal. The reverse is the case if the starting alloy contains a higher proportion of the noble metal.

This is also in accordance with the results of the microprobe analyses as shown in Fig. 1. The nickel concentration of the annealed sample (b) decreases from the surface to the interior whereas in the activated sample (c) it increases along this direction.

Similar observations have been made with Al–Ag and Al–Ni alloys which are used as catalysts for fuel cell electrodes.

4. Homogeneous alloy catalysts

The special advantage of the Raney type of noble metal catalysts described here arises from the fact that the eighth group elements belonging to the transition metals form homogeneous alloys in a broad range of composition which do not disintegrate in different phases, unlike, for instance, the Raney-nickel catalysts ($NiAl_3$ and Ni_2Al_3). This advantage is of vital importance when the alloy is composed of more than two components, such as NiPtPd, NiPtRu, etc. Not only the corresponding alloys but also the active catalysts derived from them are homogeneous, i.e. in every unit of volume ΔV there exists an analytically specified composition, assuming that ΔV is large compared with the atomic dimensions. Even with a broad spectra of other acid-insoluble transition elements such as W, Ti, Ta, Cu or Au, the homogenity remains preserved or can be enforced by a suitable annealing process.

It should be mentioned further that metals soluble in acids but insoluble in alkalis, e.g. Ni, can also be the active components if cobalt, which has to be extracted in alkali electrolytes, is chosen as an inactive partner. After the inactive component has been extracted, a completely homogeneous mixture of the catalyst is left behind which can hardly be obtained in any other manner.

Almost ideal possibilities are thus available for the preparation and development of noble metal catalysts, e.g. regulating *d*-band holes, producing and stabilizing lattice-defects, incorporating chemically effective Redox systems, or simply yielding active centres. The transport mechanisms can also be influenced by the modification of macro- and microporous structure.

It is evident that such catalysts can find application for the electrochemical oxidation of different fuels. But we have developed them for biofuel cells and therefore we will demonstrate their activity by considering glucose oxidation as an example.

4.1. *Corrosion currents of the alloy catalysts*

The ferrous metal of the alloy was extracted under drastic conditions as described in Section 2. The actual electrochemical measurements however, were conducted under mild and neutral or physiological conditions, for instance, either at room temperature or at 37°C in neutral deaerated phosphate buffer solutions at a potential of 400 mV (versus RHE).

It has been verified in all cases that under these circumstances the currents due to pure corrosion of the activated alloy catalysts were very low and negligible. Thus for example, with a Pt–Ni (1:6) and a Pt/Ta–Ni (1:6) alloy, the corrosion current densities dropped below 1 $\mu A\,cm^{-2}$ after 2 h and were not measurable thereafter. With the alloys Pt–Ni (1:4), Pt/W–Ni (1:4) and Pt/Ta–Ni (1:4), the same recorded value of 5 $\mu A\,cm^{-2}$ was obtained after 2 h. In all these cases the corrosion current densities dropped to less than 1 $\mu A\,cm^{-2}$ after 5 h, and could not be measured any further. These measurements show that the ferrous metal which is left behind in the active layer after extraction is rather inert for any corrosion in neutral media.

5. Glucose oxidation

Platinum has been preferred so far as a catalyst for glucose oxidation [2–5]. In Fig. 5 the current density-time curves for glucose oxidation on conventional platinum electrodes are compared with the curves on Pt–Ni, Pt/W–Ni and Pt/Ta–Ni electrodes prepared from alloy foils. The curves were recorded with a constant potential of 400 mV (versus RHE) at room temperature. The characteristics of the alloy catalysts are given in Table 1.

The addition of Ta and particularly W to the alloy mixture leads to a remarkable improvement of the catalytic activity as shown by curves 1 and 3 in comparison with curves 5 and 6. The activity is increased by nearly 10 to 20 times. A comparison of curves 2 and 4 shows that better results are obtained with Pt–Ni alloy having a ratio of 1:6. The activity of Pt–Ni alloys depends on the amount of nickel present in the starting alloy and

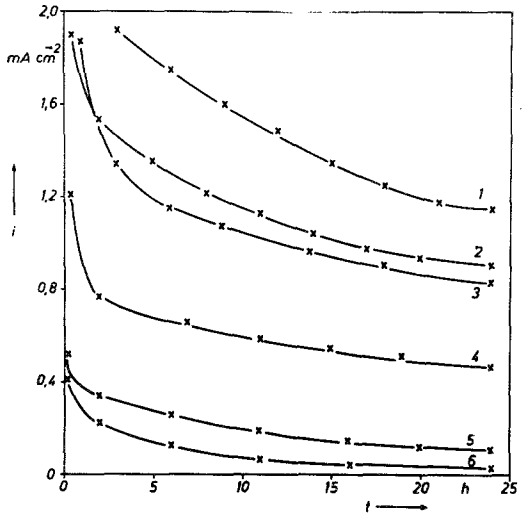

Fig. 5. Potentiostatic current density-time curves of different electrodes in deaerated phosphate buffer solution containing 0·1 M glucose; potential applied: 400 mV (RHE). Curve 1: Pt/W–Ni(1:4); curve 2: Pt–Ni(1:6); curve 3: Pt/Ta–Ni(1:4); curve 4: Pt–Ni(1:4); curve 5: conventional Pt electrode; curve 6: conventional fuel cell electrode (AA1).

the amount left behind after the activation process. As already mentioned, the 1:6 alloy has a much higher nickel content in the starting alloy and only 7·2% is left behind after activation whereas 15·9% of Ni remains behind in the 1:4 alloy. The improved performance of the 1:6 alloy (curve 2) may be due to a larger pore volume and consequently a better accessibility of the active area.

Obviously, the BET-surface area is not responsible for the improved activity of the alloy catalysts. This fact is particularly noticeable in column 6 of Table 1 in which the electrochemical active areas of the catalyst layers are mentioned. The measured BET-surface areas are expressed in column 5. The BET-surface areas of conventional platinum electrodes could not be measured because the catalysts were deposited on activated carbon. However, a minimum value of 20 $m^2\ g^{-1}$ might be assumed for both electrodes.

In the case of electrocatalysts for implantable biofuel cells it is of fundamental importance to derive maximum possible currents in a minimum volume inside the body. This can only be achieved with compact, extremely thin or foil types of electrodes which are flexible, stable and easily implantable in a small space. The new types of electrodes satisfy these requirements. When compared with the conventional electrodes they not only yield much higher currents as shown in Fig. 5, but are at the same time very compact and thin even if a margin of say up to 50 μm in thickness, is allowed for the supporting layer.

The prolonged catalytic activity of a foil electrode was investigated in a long-range test with a platinum foil electrode containing tantalum as shown in Fig. 6. Even in this case the deterioration of the current with time at constant potential cannot be overlooked, but the stability has become better by several orders of magnitude as compared with the platinum black electrode. The alloy com-

Table 1.

1 *Sample number*	*2* *Alloy composition (Atomic ratio)*	*3* *Thickness of the active layer* (μm)	*4* *Amount of the catalyst (Pt)* (mg cm^{-2})	*5* *BET-surface area* ($m^2\ g^{-1}$)	*6* *Active area* ($m^2\ cm^{-2}$)
1	Pt/W–Ni 0·9/0·1:4	15	7·5	25·2	0·189
2	Pt–Ni 1:6	14	6·0	35·9	0·215
3	Pt/Ta–Ni 0·99/0·01:4	17	9·0	14·2	0·128
4	Pt–Ni 1:4	18	10·0	19·7	0·197
5	Conventional electrode Pt–(Au)–Pt	200	15·0	At least 20	0·3
6	Conventional electrode AA1 Pt–(Ta)–Pt	150	9·0	At least 20	0·18

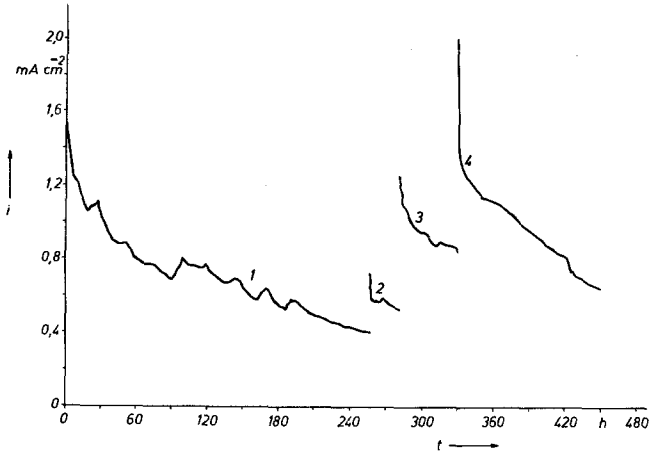

Fig. 6. Long-range test with Pt–Ta–Ni catalyst; $d = 28\ \mu m$; phosphate buffer solution with 0·1 M glucose; potential applied: $E = 400$ mV (RHE). Curve 1: at room temperature (RT); curve 2: renewal of electrolyte at RT; curve 3: temperature rise from RT to 37°C; curve 4: reactivation of the electrode.

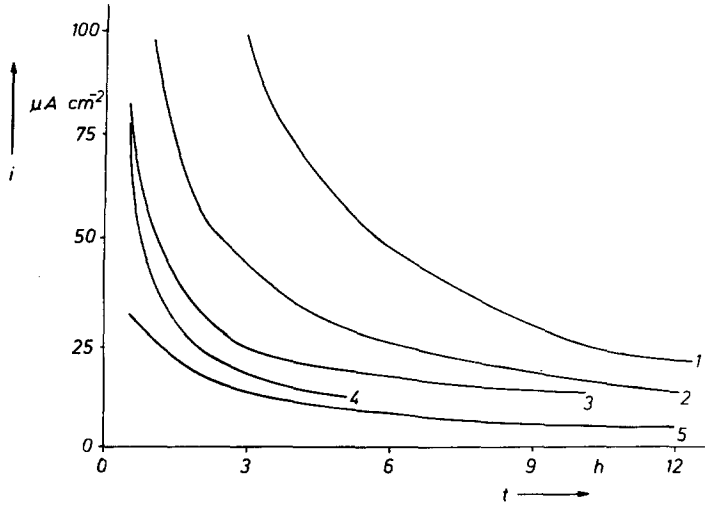

Fig. 7. Gluconic acid oxidation. Electrolyte: phosphate buffer + 2% gluconic acid saturated with Ar at RT; potential applied: $E = 400$ mV (RHE). (1) Pt–W–Ni electrode (Pt:W:Ni = 0·9:0·1:4); (2) Pt–Ni electrode (Pt:Ni = 1:4); (3) Pt–Ta–Ni electrode (Pt:Ta:Ni = 0·99:0·01:4); (4) Pt–Mo–Ni electrode (Pt:Mo:Ni = 0·8:0·2:4); (5) Pt–Ru–Ni electrode (Pt:Ru:Ni = 0·6:0·4:4). Electrodes are activated potentiostatically in 1 M H_2SO_4 at 80°C.

position is Pt : Ta : Ni = 0·98 : 0·02 : 6 and the catalyst layer contains 11·2 mg cm^{-2} of platinum.

A comparison of the partial curves 1 and 2 indicates that only a small part of the deterioration is to be attributed to the consumption of glucose.

The marked temperature effect due to the shift from 20–37°C recorded in the partial curve 3 denotes a high activation energy of the rate determining step.

The partial curve 4 shows the reactivation effect of potentiodynamic oxidation and reduction in the range between 0 and 1·6 V. However, the current drop with time after reactivation is stronger than before.

The reaction products which block the electrode surface must be considered responsible for the apparent loss of activity of the catalyst. This phenomenon was also observed in the oxidation of other organic fuels. In the case of glucose, gluconic acid was assumed to be the end product of the reaction [6]. In fact, its conversion is more difficult than that of glucose.

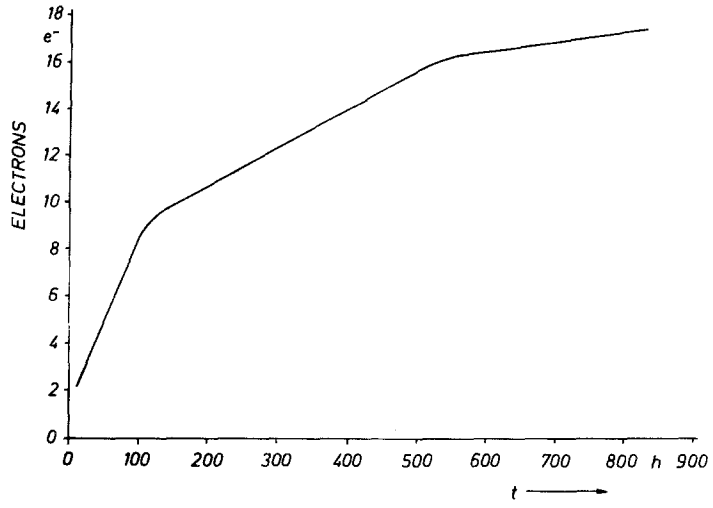

Fig. 8. Oxidation of glucose. Electron-transfer per molecule of glucose as a function of time (estimated mean value of n). Electrolyte: phosphate buffer + 0·1% glucose saturated with Ar at RT; potential applied: $E = 400$ mV (RHE).

We have therefore carried out further tests of the catalyst with gluconate as one of the inhibiting intermediate products. The behaviour of several catalysts towards gluconic acid is compared in Fig. 7. The current change with time is more drastic here than with glucose, and the currents in general are smaller. The catalyst containing tungsten is again far superior to the pure platinum catalyst. However, none of the electrodes is satisfactory where the quantitative oxidation of glucose to carbon dioxide as end product is concerned. The catalysts 1–3 of Fig. 7 are described in Table 1. The layer thickness of the catalysts in curves 4 and 5 are 13 μm and 15 μm and contain 5·7 mg cm^{-2} and 5 mg cm^{-2} of platinum respectively.

The alloy catalysts have been able so far to transfer 17 of the 24 electrons available in a glucose molecule by gradual oxidation, as shown in Fig. 8.

According to Rao and Drake [6], oxidation of glucose is supposed to proceed only to gluconic acid involving a two-electron step. But others [2, 5] have shown that the oxidation proceeds beyond the gluconic acid stage and CO_2 is obtained from glucose oxidation. However, the CO_2 evolution is not quantitative. So the number of electrons released by a glucose molecule is more than two and less than the theoretical value of 24.

Therefore, we tried to estimate experimentally the mean number of electrons. In the experiment an activated Pt–Ni (1:6) alloy catalyst was previously tested in a neutral phosphate buffer solution at 400 mV (versus RHE). The corrosion current dropped below 1 μA cm^{-2} and was not measurable after 2 h. This electrode (15 cm^2) was then brought into a phosphate buffer solution containing 0·005 M glucose (total volume 50 cm^3). Argon was passed through the electrolyte at room temperature. The electrode was maintained at 400 mV (versus RHE) and the current flowing was recorded and integrated. The initial high current of 1·6 mA cm^{-2} decreased to 250 μA cm^{-2} after 100 h; to 100 μA cm^{-2} after 500 h and to 20 μA cm^{-2} after 800 h. The experimentally derived charge was compared with the ideal charge that could be obtained. This enables us to express the mean number of electrons transfered per molecule of glucose in the course of the experiment. The n value thus obtained was 17·5.

This, however, does not imply that every molecule of glucose released 17·5 electrons. Some molecules might have been oxidized to CO_2 whilst others were only partially oxidized.

6. Design of the complete cell

Since the anode is not selective, i.e. it would take up and consume glucose and oxygen simultaneously from the surroundings, we designed the cell in such a way that the anode is arranged between two porous and selective cathodes with

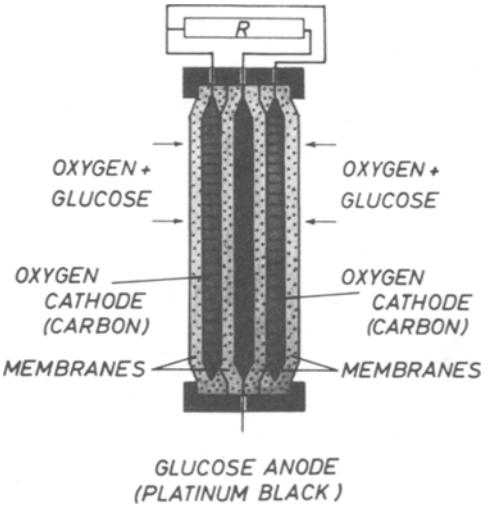

Fig. 9. Glucose oxygen fuel cell.

appropriate membranes binding them to a cell unit. Fig. 9 shows the schematic design of the cell in cross-section. Carbon and silver as cathode catalyst react with oxygen but not with glucose. The oxygen in the glucose-oxygen mixture is consumed first at the outer electrodes, so that only the glucose reaches the inner, non-selective anode [7, 8]. The active cell thickness is 500 μm approximately. The initial performance over 200 h showed that a steady power output of 5 $\mu W\,cm^{-2}$ can be obtained under physiological conditions with an external load resistance of 10 kΩ. The electrodes employed were silver cathodes and a platinum-nickel alloy catalyst as anode.

7. Concluding remarks

Where low powers such as are required to drive a cardiac pacemaker are involved, the available anode catalysts are already adequate. The oxidation to gluconic acid proceeds relatively smoothly, but further oxidation can only be conducted at lower current densities. The new catalysts display remarkable activity in oxidizing other fuels such as methanol, glycol and hydrocarbons. The investigations are under progress. The versatile nature of these foil electrodes might well be of significant importance in the fields of electrocatalysis and electroanalytical chemistry.

Acknowledgements

Our thanks are due to Miss Wiese, for experimental support; Mrs Pudritz, for carrying out the microprobe work; Miss Zwolinsky, for the scanning electron micrographs; Mr Fink, for smelting the alloys; and Mr Grüne for BET-measurements of the samples.

This work has been supported by the technical program of the Federal Department of Research and Technology of the FRG. The authors alone are responsible for the contents.

References

[1] G. Raab, personal communication; R. Dötzer and H. Kohlmüller, DOS 1909031.

[2] J. Giner and P. Malachesky, Proc. Artificial Heart Program Conf., Washington, D.C., June 1969, p. 839.

[3] S. J. Yao, M. Michuda, F. Markley and S. K. Wolfson, Jr in 'From Electrocatalysis to Fuel Cells' (G. Sandstede, Ed.), Seattle, Univ. of Washington Press (1972) p. 291.

[4] S. J. Yao, A. J. Appleby and S. K. Wolfson, Jr *Zeitschrift f. Physikalische Chemie, Neue Folge* **82** (1972) 225.

[5] B. Y. C. Wan and A. C. C. Tseung, *Medical and Biological Engineering*, January 1974, p. 14.

[6] M. L. B. Rao and R. F. Drake, *J. Electrochem. Soc.* **116, 3** (1969) 334.

[7] J. R. Rao, G. Richter, F. v. Sturm, E. Weidlich and M. Wenzel, *Biomedical Engineering* **9** (1974) 98.

[8] J. R. Rao and G. Richter, *Naturwissenschaften* **61** (1974) 200.